Inorg. Chem. **2003**, *42*, 6768–6779

Metal Complexes with a New N_4O_3 Amine Pendant-Armed Macrocyclic Ligand: Synthesis, Characterization, Crystal Structures, and Fluorescence Studies

Manuel Vicente,[†] Rufina Bastida,*[,†] Carlos Lodeiro,*[,‡] Alejandro Macías,[†] A. Jorge Parola,*[,§] Laura Valencia,[†] and Sharon E. Spey[||]

Departamento de Química Inorgánica, Facultade de Química, Universidade de Santiago de Compostela, Avda das Ciencias s/n, E-15782 Santiago de Compostela, Spain, REQUIMTE/CQFB, Faculdade de Ciências e Tecnologia, Universidade Nova de Lisboa, 2829-516 Monte de Caparica, Portugal, CQFB, Departamento de Química, Faculdade de Ciências e Tecnologia, Universidade Nova de Lisboa, 2829-516 Monte de Caparica, Portugal, and Department of Chemistry, The University of Sheffield, Sheffield, U.K. S3 7HF

Received March 6, 2003

The synthesis of a new oxaaza macrocyclic ligand, **L**, derived from *O*[1],*O*[7]-bis(2-formylphenyl)-1,4,7-trioxaheptane and tren containing an amine terminal pendant arm, and its metal complexation with alkaline earth ($M = Ca^{2+}$, Sr^{2+}, Ba^{2+}), transition ($M = Co^{2+}$, Ni^{2+}, Cu^{2+}, Zn^{2+}, Cd^{2+}), post-transition ($M = Pb^{2+}$), and Y^{3+} and lanthanide ($M = La^{3+}$, Er^{3+}) metal ions are reported. Crystal structures of $[H_2\mathbf{L}](ClO_4)_2 \cdot 3H_2O$, $[Pb\mathbf{L}](ClO_4)_2$, and $[Zn\mathbf{L}Cl](ClO_4) \cdot H_2O$ are also reported. In the [Pb**L**] complex, the metal ion is located inside the macrocyclic cavity coordinated by all N_4O_3 donor atoms while, in the [Zn**L**Cl] complex, the metal ion is encapsulated only by the nitrogen atoms present in the ligand. π–π interactions in the $[H_2\mathbf{L}](ClO_4)_2 \cdot 3H_2O$ and $[Pb\mathbf{L}](ClO_4)_2$ structures are observed. Protonation and Zn^{2+}, Cd^{2+}, and Cu^{2+} complexation were studied by means of potentiometric, UV–vis, and fluorescent emission measurements. The 10-fold fluorescence emission increase observed in the pH range 7–9 in the presence of Zn^{2+} leads to **L** as a good sensor for this biological metal in water solution.

Introduction

In most cases reactions of heterocyclic dialdehydes with tris(2-aminoethyl)amine (tren) have been shown to give cryptands[1] (L^1 in Scheme 1). Fenton et al.[2] found that the reaction of 2,6-diacetylpyridine with tren in the presence of metal templates gives a [2 + 2] pendant-armed Schiff-base macrocycle (L^2). In previous work we have reported the interesting fact that the nontemplate reaction of *O*[1],*O*[7]-bis-(2-formylphenyl)-1,4,7-trioxaheptane and tren in MeCN produced L^3, a rare example of an amino pendant-armed [1 + 1] Schiff-base macrocycle.[3] Here we report a related new functionalized pendant-armed macrocyclic ligand, **L**. This saturated ligand **L**, more stable against hydrolysis than the corresponding diiminic ligand, has been obtained by in situ reduction of L^3 with $NaBH_4$ in absence of any metal ion. Interest in pendant-armed macrocycles is growing on account of their unique coordination and structural properties,[4] their bioinorganic applications (hydrolytic enzyme models, synthetic ribonucleases, nucleobase recognition agents, oxygenase promoters),[5] their utility as contrast reagents in MRI,[6]

* To whom correspondence should be addressed. E-mail: qibastid@usc.es (R.B.); ajp@dq.fct.unl.pt (A.J.P.); lodeiro@dq.fct.unl.pt (C.L.). Phone: 00 34 981 591076 (R.B.); 00 351 21 2948300 (A.J.P.); 00 351 21 2948300 (C.L.). Fax: 00 34 981 597525 (R.B.); 00 351 21 2948385 (A.J.P.); 00 351 21 2948385 (C.L.).

[†] Universidade de Santiago de Compostela.

[‡] REQUIMTE/CQFB, Faculdade de Ciências e Tecnologia, Universidade Nova de Lisboa.

[§] CQFB, Departamento de Química, Faculdade de Ciências e Tecnologia, Universidade Nova de Lisboa.

[||] The University of Sheffield.

(1) Drew, M. G. B.; MacDowell, D.; Nelson, J. *Polyhedron* **1988**, *7(21)*, 2229−2232. (b) MacDowell, D.; Nelson, J. *Tetrahedron Lett.* **1988**, 385−386. (c) McDowell, D.; Nelson, J.; McKee, V. *Polyhedron* **1989**, *8(8)*, 1143−1145.

(2) Collinson, S. R.; Fenton, D. E. *Coord. Chem. Rev.* **1996**, *148*, 19−40.

(3) Vicente, M.; Lodeiro, C.; Adams, H.; Bastida, R.; Blas, de A.; Fenton, D. E.; Macías, A.; Rodríguez, A.; Rodríguez-Blas, T. *Eur. J. Inorg. Chem.* **2000**, 1015−1024.

(4) Rybak-Akimova, E. V.; Nazarenko, A. Y.; Silchenco, S. S. *Inorg. Chem.* **1999**, *38*, 2974−2980.

(5) Wainwright, K. P. *Adv. Inorg. Chem.* **2001**, *52*, 293−334.

(6) Botta, M. *Eur. J. Inorg. Chem.* **2000**, 399−407.

10.1021/ic034245z CCC: $25.00
Published on Web 09/26/2003

Scheme 1

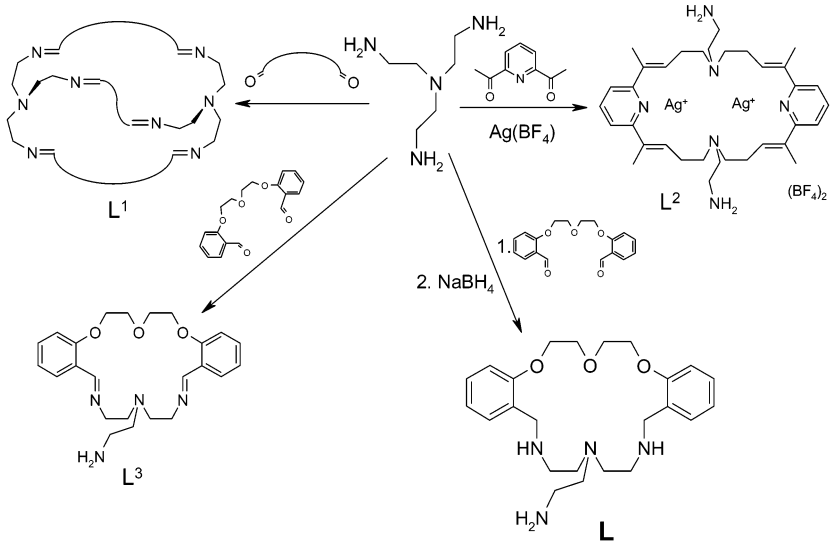

their use as tumor-directed radioisotope carriers,[7] and their ability to carry out controlled molecular movements and translocations.[8] Furthermore, this type of functionalized amino pendant-armed macrocycle provides opportunities for the synthesis of a wide range of derivatives, by a Schiff-base condensation with a suitable carbonyl compound, leading to precursors for polynuclear complexation.

Among the metal ions studied in this work, zinc is particularly important since it is an essential component of many biological substrates, as enzymes and transcription factors (for example, carbonic anhydrase, zinc finger proteins),[9,10] and has an increasing significance in several biomedical fields, as in neuroscience, immunology, cancer, etc.[11,12] Many systems have been reported in the literature to detect this metal in solution, and several research groups have been involved in the design and development of novel fluorescent probes for Zn^{2+}.[13] Particularly elegant is the work reported by Lippard and co-workers (**I**−**III**, Chart 1), in which a rhodamine or fluorescein fluorophores were linked to several types of recognition sites.[14] Between 3- and 5-fold fluorescence enhancement was observed under simulated physiological conditions upon Zn^{2+} cation binding to the sensor. Nagano and co-workers developed a new Zn^{2+} sensor (**IV**) based on fluorescein, linked to a macrocyclic system (polyamine receptor) allowing direct visible light excitation.[15] Upon addition of Zn^{2+} to **IV**, the fluorescence intensity was increased 14-fold. Previously, macrocyclic polyamine Zn^{2+} acceptors were developed by Czarnik and co-workers, in which at alkaline pH values (pH = 10) the fluorescence intensity increased also 14-fold upon coordination.[16]

Concerning macrocyclic systems provided with a flexible pendant arm, Kimura and co-workers have reported the synthesis and studies of Zn^{2+} sensors, using (anthrylmethyl)-amino (**V**) or (dimethylamino)naphthalene (**VI**) as fluorophores.[17] In those cases, upon Zn^{2+} complexation, the fluorescence intensity increased by 8-fold (**V**) and 5.2-fold (**VI**) at pH around 7.4−7.8 and 25 °C.

Experimental Section

Measurements. Elemental analyses were carried out by the University of Santiago de Compostela Microanalytical Service on Fisons Instruments EA1108 and Leco CNHS-932 microanalyzers. Infrared spectra were recorded as KBr disks using Mattson Cygnus 100 and Bio-Rad FTS 175-C spectrophotometers. Proton NMR spectra were recorded using Bruker WM-250, WM-300, and WM-

(7) Parker, D. In *Comprehensive Supramolecular Chemistry*; Atwood, J. L., Davies, J. E. D., MacNicol, D. D., Vögtle, F., Lehn, J.-M., Eds.; Pergamon: Oxford, U.K., 1996; Vol. 10, p 520.
(8) Amendola, V.; Fabbrizzi, L.; Mangano, C.; Pallavicini, P. *Struct. Bonding* **2001**, *99*, 79−115. (b) Bencini, A.; Bianci, A.; Lodeiro, C.; Masotti, A.; Parola, A. P.; Pina, F.; Seixas de Melo, J.; Valtancoli, B. *Chem. Commun*. **2000**, 1639−1640.
(9) Berg, J. M. *Acc. Chem. Res.* **1995**, *28*, 14−19.
(10) da Silva, J. J. R. F.; Williams, R. J. P. *The Biological Chemistry of Elements: The Inorganic Chemistry of Life*, 2nd ed.; Oxford University Press: Oxford, U.K., 2001; pp 315−339.
(11) Kimura, E.; Aoki, S.; Kikuta, E.; Koike, T. *Proc. Natl. Acad. Sci. U.S.A.* **2003**, *100(7)*, 3731−3736
(12) Kimura, E.; Kikuta, E. *J. Bioinorg. Chem*. **2000**, *5*, 139−155.
(13) Hendrickson, K. M.; Geue, J. P.; Wyness, O.; Lincoln, S. F.; Ward, A. D. *J. Am. Chem. Soc.* **2003**, *125*, 3889−3895. (b) Maruyama, S.; Kikuchi, K.; Hirano, T.; Urano, Y.; Nagano, T. *J. Am. Chem. Soc.* **2002**, *124*, 10650−10651. (c) Hirano, T.; Kikuchi, K.; Urano, Y.; Nagano, T. *J. Am. Chem. Soc.* **2002**, *124*, 6555−6562. (d) Ojida, A.; Mito-oka, Y.; Inoue, M.-a.; Hamachi, I. *J. Am. Chem. Soc.* **2002**, *124*, 6256−6258. (e) Jiang, P.; Chen, L.; Lin, J.; Liu, Q.; Ding, J.; Gao, X.; Guo, Z. *Chem. Commum.* **2002**, 1424−1425. (f) Fabbrizzi, L.; Licchelli, M.; Mancin, F.; Pizzeghello, M.; Rabaioli, G.; Taglietti, A.; Tecilla, P.; Tonellato, U. *Chem.*−*Eur. J.* **2002**, *8* (1), 94−101. (g) Pearce, D. A.; Jotterand, N.; Carrico, I. S.; Imperiali, B. *J. Am. Chem. Soc.* **2001**, *123*, 5160−5161. (h) Kimura, E.; Aoki, S. *Biometals* **2001**, *14* (3−4), 161−204. (i) Hirano, T.; Kikuchi, K.; Urano, Y.; Higuchi, T.; Nagano, T. *J. Am. Chem. Soc.* **2000**, *122*, 12399−12400. (j) Walkup, G. K.; Imperiali, B. *J. Am. Chem. Soc.* **1997**, *119*, 3443−3450.
(14) Burdette, S. C.; Frederickson, C. J.; Bu, W.; Lippard, S. J. *J. Am. Chem. Soc.* **2003**, *125*, 1778−1787. (b) Burdette, S. C.; Bu, W.; Lippard, S. J. *Inorg. Chem.* **2002**, *41*, 6816−6823. (c) Burdette, S. C.; Walkup, G. K.; Spingler, B.; Tsien, R. Y.; Lippard, S. J. *J. Am. Chem. Soc.* **2001**, *123*, 7831−7841. (d) Walkup, G. K.; Burdette, S. C.; Lippard, S. J.; Tsien, R. Y. *J. Am. Chem. Soc.* **2000**, *122*, 5644−5645.
(15) Hirano, T.; Kikuchi, K.; Urano, Y.; Higuchi, T.; Nagano, T. *Angew. Chem. Int. Ed.* **2000**, *39(6)*, 1052−1054.
(16) Akkaya, E. U.; Huston, M. E.; Czarnik, A. W. *J. Am. Chem. Soc.* **1990**, *112*, 3590−3593.
(17) Koike, T.; Abe, T.; Takahashi, M.; Ohtani, K.; Kimura, E.; Shiro, M. *J. Chem. Soc., Dalton Trans.* **2002**, 1764−1768. (b) Aoki, S.; Kaido, S.; Fujioka, H.; Kimura, E. *Inorg. Chem.* **2003**, *42*, 1023−1030.

Chart 1

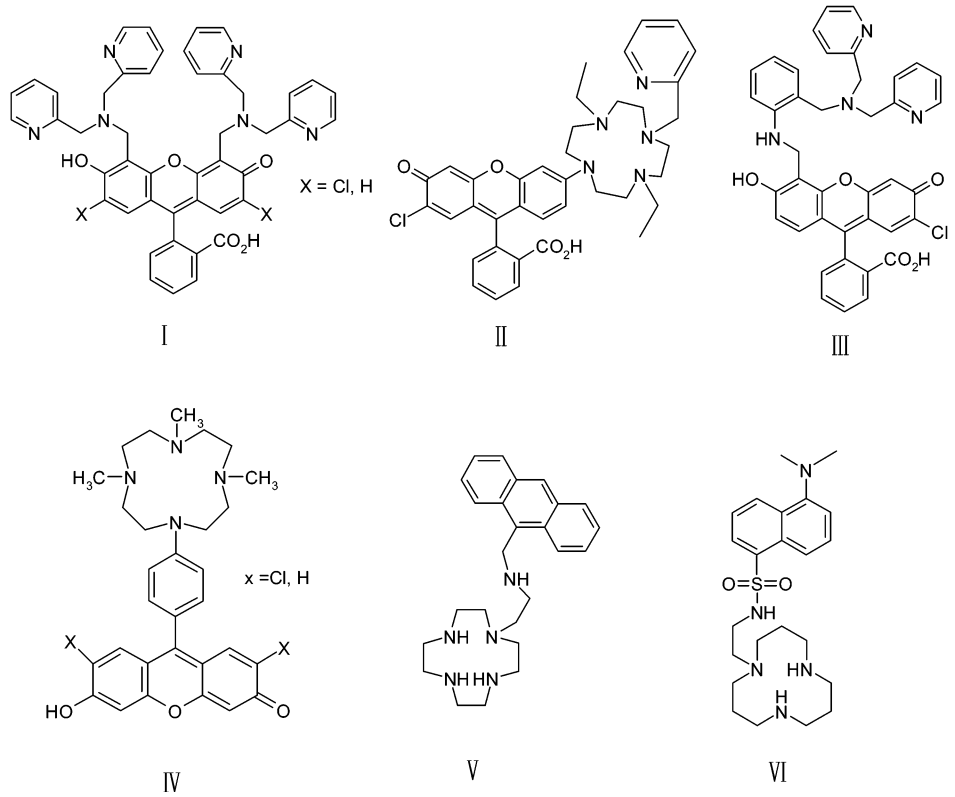

500 spectrometers. Positive ion FAB mass spectra were recorded on a Kratos MS50TC spectrometerusing a 3-nitrobenzyl alcohol (MNBA) matrix. Electronic impact spectra were determined on a HP 5988-A spectrometer. Conductivity measurements were carried out in 10^{-3} mol dm^{-3} MeCN solutions at 20°C using a WTW LF-3 conductivimeter.

Potentiometric Measurements. Equilibrium constants for protonation and complexation reactions with **L** were determined by pH-metric measurements in 0.15 mol dm^{-3} NaCl at 298.0 ± 0.1 K, by using potentiometric equipment similar to the one described in ref 18. The glass electrode was calibrated against a Ag/AgCl reference electrode by titrating known amounts of HCl with CO_2-free standard 0.1 mol dm^{-3} NaOH solutions and determining the equivalence point by Gran's method.[19] This allows determination of the standard potential $E°$ and the ionic product of water in the medium used. Concentrations of **L** in the range $5 \times 10^{-4}-7 \times 10^{-4}$ mol dm^{-3} had to be used to avoid precipitation during titrations. The concentration of metal ions was in the same range varying the metal to ligand molar ratio from 0.7:1 to 0.9:1. Three titration experiments (about 100 data points each) were performed in the pH range 2.0−10.0. The computer program HYPERQUAD[20] was used to calculate the equilibrium constants from the emf data. All titrations were treated either as single sets or as separated entities, for each system without significant variations in the values of the constants determined.

Spectrophotometric and Spectrofluorometric Measurements. Absorption spectra were recorded on a Shimadzu spectrophotometer and fluorescence emission on a SPEX Fluorolog spectrofluorometer. HCl and NaOH were used to adjust the pH values that were measured on a Metrohm 713 pH meter. All measurements were made in 0.15 mol dm^{-3} NaCl.

Chemicals and Starting Materials. O^1,O^7-Bis(2-formylphenyl)-1,4,7-trioxaheptane was prepared according to a literature method;[21] tris(2-aminoethyl)amine and the metal salts were commercial products (from Alfa, Fluka, and Aldrich) used without further purification. Solvents were of reagent grade purified by the usual methods.

Caution! *Perchlorate salts are potentially explosive. Only small amounts of material should be prepared and handled with great care; particular caution must be exercised when they are heated in vacuo.*

Synthesis of Macrocycle L. The reaction was carried out according to a modification of a literature method.[22] Tris(2-aminoethyl)amine (2.0 mmol) in MeOH (20 mL) was added to a boiling solution of O^1,O^7-bis(2-formylphenyl)-1,4,7-trioxaheptane in MeOH (100 mL). The resulting mixture was refluxed for 30 min and cooled, and then solid $NaBH_4$ (10 mmol) was carefully added portionwise with stirring. After 2 h, the solution was concentrated to approximately 60 mL and the volume was increased 2-fold by addition of crushed ice. Stirring was continued at room temperature overnight in an open beaker. Solution was extracted with chloroform, and the chloroform extract was dried over anhydrous sodium sulfate and then taken to dryness on a rotary evaporator. The crude product was obtained as a light brown oil soluble in MeOH, EtOH, MeCN, DMSO, and $CHCl_3$ and insoluble in water and Et_2O. Anal. Calcd for $C_{24}H_{36}N_4O_3 \cdot CH_3OH$: C, 65.20; H, 8.75; N, 12.15. Found: C, 65.45; H, 8.95; N, 12.20. Yield: 65%.

(18) Bencini, A.; Bianchi, A.; Castello, M.; Dapporto, P.; Faus, J.; Garcia-España, E.; Micheloni, M.; Paoletti, P.; Paoli, P. *Inorg. Chem.* **1989**, *28*, 3175−3181.
(19) (a) Gran, G. *Analyst* (*London*) **1952**, *77*, 661−671. (b) Rossotti, F. J.; Rossotti, H. *J. Chem. Educ.* **1965**, *42*, 375−378.
(20) Gans, P.; Sabatini, A.; Vacca, A. *Talanta* **1996**, *43*, 1739−1753.
(21) Adam, K. R.; Leong, A. J.; Lindoy, L. F.; Lip, H. C.; Skelton, B. W.; White, A. H. *J. Am. Chem. Soc.* **1983**, *105*, 4645−4651.
(22) Davis, C. A.; Duckworth, P. A.; Lindoy, L. F., Moody, W. E. *Aust. J. Chem.* **1995**, *48*, 1819−1825.

IR (NaCl window): 3310 br, 1664 w [$\delta(NH_2)$], 1600 [ν(C=C)] cm^{-1}. ^1H NMR (500 MHz, $CDCl_3$): δ/ppm 7.15−7.08 (m, 4H, H_e, H_g), 6.84−6.74 (m, 4H, H_f, H_d), 4.11−4.07 (m, 4H, H_b, $H_{b'}$), 3.92−3.89 (m, 4H, H_a, $H_{a'}$), 3.72 (s, 4H, H_i, $H_{i'}$), 2.86−2.68 (s, br, 2H, H_o), 2.55 (t, J = 5.8 Hz, 4H, H_k, $H_{k'}$), 2.47 (t, J = 6.0 Hz, 2H, H_n), 2.42 (t, J = 5.8 Hz, 4H, H_l, $H_{l'}$), 2.19 (t, J = 6.0 Hz, 2H, H_m). ^{13}C NMR (500 MHz, $CDCl_3$): δ/ppm 156.5 (C_c), 130.0 (C_g), 128.3 (C_h), 127.8 (C_e), 120.2 (C_f), 111.2 (C_d), 69.8 (C_a), 67.8 (C_b), 57.4 (C_m), 53.9 (C_l), 49.2 (C_i), 46.1 (C_k), 39.1 (C_n). MS (FAB:MNBA): m/z 429 (100%), [**L** + H]$^+$. MS (EI): P^+ 398, [**L** − CH_2NH_2]$^+$.

The water-soluble tetrahydrobromide salt was obtained by addition of HBr to an ethanolic solution of **L**. The gray precipitate was filtered out, washed with absolute ethanol, dried in vacuo, and characterized. Anal. Calcd for $C_{24}H_{36}N_4O_3 \cdot 4HBr \cdot 4H_2O$: C, 34.95; H, 5.85; N, 6.80. Found: C, 35.65; H, 5.25; N, 6.55. IR (KBr disk): 3417 br, 1605 [ν(C=C)] cm^{-1}. ^1H NMR (250 MHz, D_2O): δ/ppm 7.44−7.30 (m, 4H, H_e, H_g), 7.07−6.96 (m, 4H, H_f, H_d), 4.27−4.22 (m, 4H, H_b, $H_{b'}$), 4.20 (s, 4H, H_i, $H_{i'}$), 3.99−3.93 (m, 4H, H_a, $H_{a'}$), 3.12 (t, J = 6.3 Hz, 4H, H_k, $H_{k'}$), 2.98 (*pseudo* t, 2H, H_n), 2.83 (t, J = 6.3 Hz, 4H, H_l, $H_{l'}$), 2.75 (*pseudo* t, 2H, H_m). MS (FAB:MNBA): m/z 429, [**L** + H]$^+$ (100%), 509, [**L** + HBr]$^+$, 590, [**L** + $(HBr)_2$]$^+$. Crystals suitable for a X-ray crystallographic study were obtained by slow diffusion of a diluted ethanolic solution of **L** into a $Ba(ClO_4)_2$ water solution.

Metal Complexes of Macrocycle L. General Procedure. This reaction was attempted with $M(ClO_4)_2 \cdot xH_2O$ (M = Ca^{2+}, Sr^{2+}, Ba^{2+}, Co^{2+}, Ni^{2+}, Cu^{2+}, Zn^{2+}, Cd^{2+} and Pb^{2+}), $M(ClO_4)_3 \cdot xH_2O$ (M = La^{3+}, Er^{3+}), and $M(NO_3)_3 \cdot xH_2O$ (M = La^{3+}, Er^{3+}, Y^{3+}). The appropriate metal salt (0.40 mmol) was dissolved in absolute ethanol (10 mL) and slowly added to a stirred boiling solution of the ligand **L** (0.40 mmol) in the same solvent. The resulting mixture was refluxed for 3 h. A precipitate was observed, which was collected by filtration, washed with absolute ethanol, dried in vacuo, and characterized as the perchlorate complex in the case of Zn^{2+}, Cd^{2+}, Ca^{2+}, Sr^{2+}, and Ba^{2+}. In the reactions with the other salts this first precipitate was removed by filtration. The solution was concentrated to a volume of ca. 10 mL in a rotary evaporator and was left to crystallize at rt (room temperature) for 24 h. A crystalline precipitate of the Co^{2+}, Ni^{2+}, and Cu^{2+} perchlorate complexes was collected by filtration, washed with cold absolute ethanol, and dried in vacuo. In the reactions with La^{3+}, Er^{3+}, and Y^{3+} salts no analytically pure products could be isolated.

[CaL](ClO$_4$)$_2$·2H$_2$O (1). Anal. Calcd for $C_{24}H_{40}N_4O_{13}Cl_2Ca$: C, 40.95; H, 5.75; N, 7.95. Found: C, 41.25; H, 5.80; N, 7.60. Yield: 15%. IR (KBr): 2937, 2877 [$\nu(CH_2)$], 1603 [ν(C=C)], 1142, 1120, 1090, 636, 627 [$\nu(ClO_4^-)$] cm^{-1}. MS (FAB:MNBA): m/z 429, [**L** + H]$^+$, 567, [Ca**L**(ClO_4)]$^+$, isotopic patterns correspond to the proposed formulation. Λ_M (CH_3CN): 130 Ω^{-1} cm^2 mol^{-1}. The white complex was found to be soluble in MeCN, DMSO, and DMF, moderately soluble in absolute EtOH, MeOH, water, and $CHCl_3$, and insoluble in Et_2O.

[SrL](ClO$_4$)$_2$ (2). Anal. Calcd for $C_{24}H_{36}N_4O_{11}Cl_2Sr$: C, 40.30; H, 5.05; N, 7.85. Found: C, 40.45; H, 5.50; N, 7.75. Yield: 32%. IR (KBr): 3350, 3296, 3281 [ν(NH)], 2933, 2856 [$\nu(CH_2)$], 1598 [ν(C=C)], 1111, 1065, 621 [$\nu(ClO_4^-)$] cm^{-1}. MS (FAB:MNBA): m/z 429, [**L** + H]$^+$, 615, [Sr**L**(ClO_4)]$^+$ (100%). Λ_M (CH_3CN): 208 Ω^{-1} cm^2 mol^{-1}. The white complex was found to be soluble in DMSO and DMF, moderately soluble in absolute EtOH, MeOH, MeCN, and water, and insoluble in Et_2O and $CHCl_3$.

[BaL](ClO$_4$)$_2$·0.5H$_2$O (3). Anal. Calcd for $C_{24}H_{37}N_4O_{11.5}Cl_2Ba$: C, 37.25; H, 4.85; N, 7.25. Found: C, 37.60; H, 5.05; N, 7.20. Yield: 52%. IR (KBr): 3354, 3296 [ν(NH)], 2941, 2860 [$\nu(CH_2)$], 1598 [ν(C=C)], 1112, 1061, 624 [$\nu(ClO_4^-)$] cm^{-1}. MS (FAB: MNBA): m/z 429, [**L** + H]$^+$, 665, [Ba**L**(ClO_4)]$^+$ (100%). Λ_M (CH_3CN): 157 Ω^{-1} cm^2 mol^{-1}. The white complex was found to be soluble in MeCN, DMSO, and DMF, moderately soluble in absolute EtOH, MeOH, water, and $CHCl_3$, and insoluble in Et_2O.

[CoL](ClO$_4$)$_2$·3EtOH (4). Anal. Calcd for $C_{30}H_{54}N_4O_{14}Cl_2Co$: C, 43.70; H, 6.60; N, 6.80. Found: C, 44.25; H, 6.05; N, 7.05. Yield: 28%. IR (KBr): 3257 [ν(NH)], 2937, 2879 [$\nu(CH_2)$], 1598 [ν(C=C)], 1096, 625 [$\nu(ClO_4^-)$] cm^{-1}. Λ_M (CH_3CN): 246 Ω^{-1} cm^2 mol^{-1}. The brown complex was found to be soluble in MeCN, absolute EtOH, DMSO, and DMF, moderately soluble in MeOH and water, and insoluble in Et_2O and $CHCl_3$.

[NiL](ClO$_4$)$_2$·EtOH·0.5H$_2$O (5). Anal. Calcd for $C_{26}H_{43}N_4O_{12.5}Cl_2Ni$: C, 42.10; H, 5.85; N, 7.55. Found: C, 42.55; H, 5.75; N, 7.45**.** Yield: 31%. IR (KBr): 3350 vw, 3288 vw [ν(NH)], 2934, 2879 [$\nu(CH_2)$], 1656 w [$\delta(NH_2)$], 1598 [ν(C=C)], 1098 br, 625 [$\nu(ClO_4^-)$] cm^{-1}. MS (FAB:MNBA): m/z 485, [Ni**L** + H]$^+$, 585, [Ni**L**(ClO_4)]$^+$ (100%), isotopic patterns correspond to the proposed formulation. Λ_M (CH_3CN): 254 Ω^{-1} cm^2 mol^{-1}. The green complex was found to be soluble in MeCN, DMSO, and DMF, moderately soluble in absolute EtOH and water, and insoluble in Et_2O, MeOH, and $CHCl_3$.

[CuL](ClO$_4$)$_2$·3H$_2$O (6). Anal. Calcd for $C_{24}H_{42}N_4O_{14}Cl_2Cu$: C, 38.70; H, 5.70; N, 7.50. Found: C, 38.75; H, 5.60; N, 7.35. Yield: 40%. IR (KBr): 3342 vw, 3265 [ν(NH)], 2969, 2933, 2879 [$\nu(CH_2)$], 1650 br w [$\delta(NH_2)$], 1597 [ν(C=C)], 1092, 625 [$\nu(ClO_4^-)$] cm^{-1}, MS (FAB:MNBA): m/z 491, [Cu**L**]$^+$, 592, [Cu**L**(ClO_4) + H]$^+$, isotopic patterns correspond to the proposed formulation. Λ_M (CH_3CN): 227 Ω^{-1} cm^2 mol^{-1}. The blue complex was found to be soluble in MeCN, DMSO, and DMF, moderately soluble in absolute EtOH, MeOH, and water, and insoluble in Et_2O and $CHCl_3$.

[ZnL](ClO$_4$)$_2$·EtOH·H$_2$O (7). Anal. Calcd for $C_{26}H_{44}N_4O_{13}Cl_2Zn$: C, 41.25; H, 5.85; N, 7.40. Found: C, 41.55; H, 5.60; N, 7.40. Yield: 78%. IR (KBr): 3281 vw, 3282 [ν(NH)], 2933, 2879 [$\nu(CH_2)$], 1644 br w [$\delta(NH_2)$], 1598 [ν(C=C)], 1100, 621 [$\nu(ClO_4^-)$] cm^{-1}. MS (FAB:MNBA): m/z 491, [Zn**L**]$^+$, 591, [Zn**L**(ClO_4)]$^+$, isotopic pattern corresponds to the proposed formulation. Λ_M (CH_3CN): 254 Ω^{-1} cm^2 mol^{-1}. The light yellow complex was found to be soluble in MeCN, DMSO, and DMF, moderately soluble in absolute EtOH, MeOH, and water, and insoluble in Et_2O and $CHCl_3$. Crystals suitable for a X-ray crystallographic study were obtained by slow diffusion of a diluted ethanolic solution of $Zn(ClO_4)_2 \cdot 6H_2O$ into a **L**·4HCl water solution.

[CdL](ClO$_4$)$_2$·3H$_2$O (8). Anal. Calcd for $C_{24}H_{42}N_4O_{14}Cl_2Cd$: C, 36.30; H, 5.35; N, 7.05. Found: C, 36.55; H, 5.05; N, 6.95. Yield: 26%. IR (KBr): 3273 [ν(NH)], 2933, 2879 [$\nu(CH_2)$], 1602 [ν(C=C)], 1100 br, 625 [$\nu(ClO_4^-)$] cm^{-1}. MS (FAB:MNBA): m/z 641 [Cd**L**(ClO_4)]$^+$, isotopic pattern corresponds to the proposed formulation. Λ_M (CH_3CN): 235 Ω^{-1} cm^2 mol^{-1}. The white complex was found to be soluble in MeCN, DMSO, and DMF, moderately soluble in absolute EtOH, MeOH, and water, and insoluble in Et_2O and $CHCl_3$.

[PbL](ClO$_4$)$_2$·0.5EtOH (9). Anal. Calcd for $C_{24}H_{39}N_4O_{11.5}Cl_2Pb$: C, 35.00; H, 4.60; N, 6.55. Found: C, 35.25; H, 4.45; N, 6.50. Yield: 51%. IR (KBr): 3346, 3288, 3265, 3246 [ν(NH)], 2925, 2875 [$\nu(CH_2)$], 1602 [ν(C=C)], 1100, 621 [$\nu(ClO_4^-)$] cm^{-1}. MS (FAB:MNBA): m/z 429, [**L** + H]$^+$, 636, [Pb**L**]$^+$, 735, [Pb**L**(ClO_4)]$^+$ (100%), isotopic patterns correspond to the proposed formulation. Λ_M (CH_3CN): 261 Ω^{-1} cm^2 mol^{-1}. The white complex was found to be soluble in MeCN, absolute EtOH, DMSO, and DMF, moderately soluble in MeOH and Et_2O, and insoluble in water and $CHCl_3$. Recrystallization from MeCN resulted in the formation of crystals suitable for a X-ray crystallographic study.

Table 1. Crystal Data and Structure Refinement of $[H_2\mathbf{L}](ClO_4)_2\cdot 3H_2O$, $[Pb\mathbf{L}](ClO_4)_2$, and $[Zn\mathbf{L}Cl](ClO_4)\cdot H_2O$

	$[H_2\mathbf{L}](ClO_4)_2\cdot 3H_2O$	$[Pb\mathbf{L}](ClO_4)_2$	$[Zn\mathbf{L}Cl](ClO_4)\cdot H_2O$
empirical formula	$C_{24}H_{44}Cl_2N_4O_{14}$	$C_{24}H_{36}Cl_2N_4O_{11}Pb$	$C_{24}H_{38}Cl_2N_4O_8Zn$
fw	684.54	834.66	646.85
T, K	150(2)	293(2)	293(2)
wavelength, Å	0.710 73	0.710 73	1.541 84
cryst syst	triclinic	monoclinic	monoclinic
space group	$P\bar{1}$	$P2_1/c$	$P2_1/n$
a, Å	9.650(7)	9.6686(15)	13.815(2)
b, Å	10.244(7)	13.225(2)	14.774(5)
c, Å	17.201(12)	23.633(4)	15.133(4)
α, deg	90.000(14)		
β, deg	90.000(12)	90.254(3)	109.104(13)
γ, deg	71.895(12)		
V, Å^3	1616.2(19)	3022.0(8)	2918.7(13)
Z, d_{cald} (g cm^{-3})	2, 1.405	4, 1.835	4, 1.472
abs coeff, mm^{-1}	0.271	5.823	3.300
final R indices[a]	$R_1 = 0.0839$	$R_1 = 0.0296$	$R_1 = 0.0706$
$[I > 2\sigma(I)]$	$wR_2 = 0.2297$	$wR_2 = 0.0679$	$wR_2 = 0.1847$

[a] $R_1 = \Sigma||F_o| - |F_c||/\Sigma|F_o|$; $wR_2 = [\Sigma w(F_o^2 - F_c^2)^2/\Sigma w(F_o^2)^2]^{1/2}$.

X-ray Crystal Structure Determinations. Three colorless crystals, $[H_2\mathbf{L}](ClO_4)_2\cdot 3H_2O$, $[Pb\mathbf{L}](ClO_4)_2$, and $[Zn\mathbf{L}Cl](ClO_4)\cdot H_2O$, crystallized from ethanol/water, MeCN, and ethanol/water, respectively, were used for the structure determinations. Data collected were measured on a Bruker Smart CCD area detector ($[H_2\mathbf{L}](ClO_4)_2\cdot 3H_2O$ and $[Pb\mathbf{L}](ClO_4)_2$) with an Oxford Cryosystems low-temperature system for $[H_2\mathbf{L}](ClO_4)_2\cdot 3H_2O$ and on an Enraf-Nonius Cad4 diffractometer equipped with a graphite monochromator for $[Zn\mathbf{L}Cl](ClO_4)\cdot H_2O$. Crystal data, data collection parameters, and convergence results are listed in Table 1. All reflections measured were corrected for Lorentz and polarization effects and for absorption by empirical[23] (for $[H_2\mathbf{L}](ClO_4)_2\cdot 3H_2O$ and $[Pb\mathbf{L}](ClO_4)_2$) and *ψ*-scan[24] (for $[Zn\mathbf{L}Cl](ClO_4)\cdot H_2O$) methods. The structures were solved by direct methods ($[H_2\mathbf{L}](ClO_4)_2\cdot 3H_2O$) and by the heavy atom method ($[Pb\mathbf{L}](ClO_4)_2$ and $[Zn\mathbf{L}Cl](ClO_4)\cdot H_2O$) and refined by full-matrix least-squares methods on F^2. The amine and water hydrogen atoms were located on a Fourier map. All other hydrogen atoms were placed geometrically and refined with a riding model (including torsional freedom for methyl groups) and with U_{iso} constrained to be 1.2 (1.5 for methyl groups) times U_{eq} of the carrier atom.

The perchlorate anions were found to be disordered in all three structures and were refined using different models. Also for $[H_2\mathbf{L}](ClO_4)_2\cdot 3H_2O$, one of the additional hydrogens has been placed on the nitrogen atom (N4) and the second has been modeled to be disordered (53.5:46.5%) between N1 and N3. The water molecule (O2S) between these two nitrogen atoms can form hydrogen bond interactions to them (O2S−N1 = 2.781 Å and O2S−N3 = 2.752 Å), and one of the hydrogen atoms on this water molecule is disordered appropriately to fit in with the disordered hydrogen on the nitrogen atoms. Program used to solve and refine the structures: SHELX-97.[25] Molecular graphics: ORTEP-3.[26] Software used to prepare material for publication: SHELX-97.

Results and Discussion

Ligand **L** was prepared by direct cyclocondensation between O^1,O^7-bis(2-formylphenyl)-1,4,7-trioxaheptane and tren in methanol followed by an in situ reduction with $NaBH_4$. Furthermore, the water-soluble tetrahydrobromide salt was also obtained. The FAB mass spectrum of **L**·MeOH features the parent peak at *m*/*z* 429 assigned to the molecular ion $[\mathbf{L} + H]^+$ providing strong evidence that the macrocycle is the 1:1 condensation product. The IR spectrum of **L** (NaCl windows) shows no bands assignable to carbonyl or azomethine groups. Amine stretches of the −NH and $-NH_2$ groups are unassignable because there is an intense broad band centered at ca. 3310 cm^{-1} consistent with the presence of methanol as suggested from the microanalytical data.

NMR Spectra of L. The ^{1}H and ^{13}C NMR spectra of **L**·MeOH were recorded in $CDCl_3$ and CD_3CN and confirm the integrity of the ligand and its stability in solution. Spectral data are listed in the Experimental Section and in Table S1 (Supporting Information), respectively. No change in the spectra was observed after 72 h. The spectra show that the two halves of the macrocyclic ring are chemically equivalent; i.e., there is a C_2 axis that crosses the middle ether oxygen and the tertiary nitrogen atom as shown by the ^{13}C spectrum that exhibits only 11 resonances for the carbons of the macrocyclic backbone and two for carbons of the pendant arm. In the proton NMR spectra the OCH_2CH_2O chains give rise to two multiplets suggesting the magnetic inequivalence of the geminal hydrogen pairs caused by restricted rotation about the C−C bonds.[27,28] However, in the spectrum registered in $CDCl_3$, H_i and $H_{i'}$ give rise to a singlet and H_k, $H_{k'}$, H_l, $H_{l'}$, H_m, and H_n to four triplets, indicating that this part of the macrocycle is less rigid. Assignment of the broad NH signals was confirmed by deuterium exchange when D_2O was added to the solutions.

Metal Complexes of L. Complexation reactions between the ligand **L** with hydrated metal salts in refluxing ethanol in a 1:1 molar ratio were carried out to investigate the coordination capability of the ligand. Analytically pure products were obtained and formulated as $M(ClO_4)_2\cdot x$EtOH·

(23) Sheldrick, G. M. *Sadabs, Program for Empirical Absoption Correction of Area Detector Data*; University of Göttingen: Göttingen, Germany, 1996.
(24) North, A. C. T.; Phillips, D. C.; Mathews, F. S. *Acta Crystallogr.* **1968,** *A24*, 351.
(25) Sheldrick, G. M. *SHELX-97, An Integrated System for Solving and Refining Crystal Structures from Diffraction Data*; University of Göttingen: Göttingen, Germany, 1997.
(26) Farrugia, L. J. *J. Appl. Crystallogr.* **1997**, *30*, 565.
(27) Bailey, N. A.; Rodríguez de Barbarín, C. O.; Fenton, D. E.; Hellier, P. C.; Hempstead, P. D.; Kanesato, M.; Leeson, P. B. *J. Chem. Soc., Dalton Trans.* **1995**, 765−770.
(28) Adams, H.; Bailey, N. A.; Dwyer, M. J. S.; Fenton, D. E.; Hellier, P. C.; Hempstead, P. D.; Latour, J. M. *J. Chem. Soc., Dalton Trans.* **1993**, 1207−1216.

yH$_2$O for M = Ca^{2+}, Sr^{2+}, Ba^{2+}, Co^{2+}, Ni^{2+}, Cu^{2+}, Zn^{2+}, Cd^{2+}, and Pb^{2+}. Attempts to obtain Y^{3+} or Ln^{3+} complexes were unsuccessful. This contrasts with the results previously reported for the diiminic macrocycle L[3], where complexes for Cd^{2+}, and Ln^{3+} (Er^{3+} and Dy^{3+}) have been obtained.[3]

The FAB mass spectra of the complexes feature peaks corresponding to the free ligand and the fragments [M**L**]$^+$ and [M**L**(ClO$_4$)]$^+$. The IR spectra of the complexes were recorded using KBr disks, and all show similar features. Amine stretches appear in the region 3350−3250 cm^{-1}. Absorptions attributable to ionic perchlorate were found approximately at 1095 and 624 cm^{-1}.[29,30] Except in the case of the Ca^{2+}, Sr^{2+}, and Ba^{2+} complexes, the lack of splitting of these bands suggests that perchlorate anions are not coordinated. The highest energy bands in complexes **1**−**3** complexes comprise three well-resolved maxima at ca. 1140, 1110, and 1060 cm^{-1} indicating the presence of coordinated perchlorate groups. The molar conductivities of the complexes in MeCN fall within the range reported for 2:1 electrolytes, except in the Sr^{2+} complex that lies between 2:1 and 1:1 electrolytes and, Ba^{2+} and Ca^{2+} complexes that fall in the range characteristic of 1:1.[31]

NMR Spectra of the Diamagnetic Complexes. ^{1}H NMR spectra of Ca^{2+}, Sr^{2+}, Ba^{2+}, Zn^{2+}, Cd^{2+}, and Pb^{2+} complexes were recorded immediately after dissolution in CD$_3$CN. After 24 h the spectra registered showed no significant changes. The spectrum for the Sr^{2+} complex was recorded in DMSO-d_6 due to its low solubility in MeCN; this spectrum only features free ligand signals indicating demetalation processes in DMSO. The spectra for Cd^{2+}, Ba^{2+}, and Zn^{2+} complexes could not be fully assigned. Ba^{2+} and Cd^{2+} complexes exhibit broad and poorly resolved signals that could stem from the presence of different conformers in solution or species with different coordination environments. In the Ba^{2+} spectrum when temperature is lowered to 238 K, a large number of well-resolved signals appear which could correspond to two species in equilibrium, one of them the majority. However, in the Cd^{2+} spectrum at the same temperature, only the aromatic signals were well resolved. In the case of the Zn^{2+} complex, the spectrum at 298 K shows many and complex signals. Furthermore, the ^{13}C NMR spectrum gives rise to more signals than would be expected, suggesting again the presence of related conformers in solution or the instability of the complex in CD$_3$CN.

The spectral data for Ca^{2+} and Pb^{2+} complexes are listed in Table S1 (see Supporting Information). As in the free ligand, both spectra present chemical equivalence between the two halves of the macrocyclic ring. However, signals are generally shifted to low field when compared with the free ligand due to the coordination to the metal atoms (see Figure 1; the assignment corresponds to the labels in Chart 2). The assignment of the proton signals was based upon standard 2D homonuclear (COSY) and ^{1}H/^{13}C heteronuclear spectra (HMQC). The resolution of geminal protons into separate multiplets shows that the $\delta \leftrightarrow \lambda$ conformational

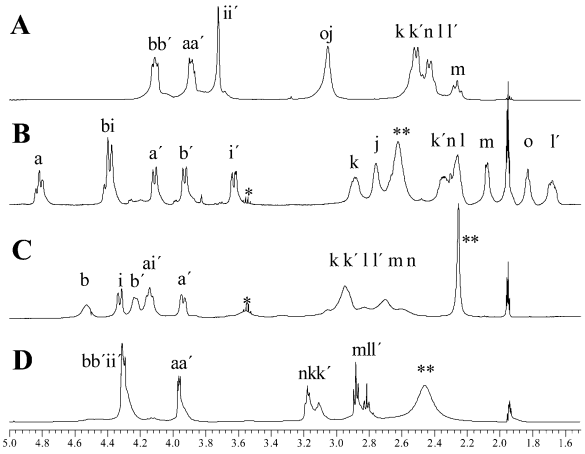

Figure 1. ^{1}H NMR spectra (500 MHz) in CD$_3$CN of **L**·MeOH (A), [Ca**L**](ClO$_4$)$_2$·2H$_2$O (B), [Pb**L**](ClO$_4$)$_2$·0.5EtOH (C), and [Pb$_2$**L**](ClO$_4$)$_4$ (D). The resonances labeled with * and ** refer to ethanol and water protons, respectively.

Chart 2

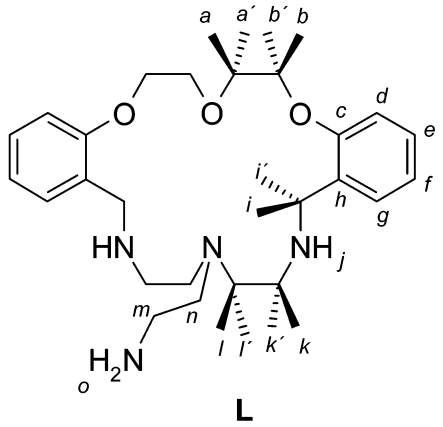

L

forms of the five-membered rings formed by the metal with the respective OCH$_2$CH$_2$O and NCH$_2$CH$_2$N chains are not rapidly interconverting in solution on the time scale of the NMR experiment.[32−34] Upon complexation of the macrocycle with calcium, H$_i$ and H$_{i'}$ resonances, which appear as a singlet in the spectrum of the free ligand, give rise to a double doublet at δ 3.61 and a broad signal at δ 4.42−4.32 overlapped with H$_b$ resonance. H$_i$ and H$_{i'}$ are inequivalent and form the AB part of an ABX spin system, where X is the vicinal amine hydrogen H$_j$. This coupling and the H$_n$−H$_o$ coupling were verified by the COSY spectrum. In the [Pb**L**](ClO$_4$)$_2$·0.5EtOH complex geminal coupling between H$_i$ and H$_{i'}$ is observed, whereas vicinal couplings between H$_j$ and H$_{i \text{ or } i'}$ or between H$_o$ and H$_n$ are not.

Proton NMR titrations of macrocycle **L** with M(ClO$_4$)$_2$·xH$_2$O (M = Ca^{2+}, Ba^{2+}, Zn^{2+}, Cd^{2+}, and Pb^{2+}) were performed in CD$_3$CN. In all spectra, resonances for the free ligand gradually diminish in intensity, while resonances for the complex grow indicating that complexation is kinetically

(29) Rosenthal, M. R. *J. Chem. Educ.* **1973**, *50*, 331−335.
(30) Pavkovic, S. F.; Meek, D. W. *Inorg. Chem.* **1965**, *4*, 1091−1098.
(31) Geary, W. J. *Coord. Chem. Rev.* **1971**, *7*, 81−122.
(32) Bryant, L. H.; Lachgar, A.; Coates, K. S.; Jackels, S. C. *Inorg. Chem.* **1994**, *33*, 2219−2226.
(33) Bryant, L. H.; Lachgar, A.; Jackels, S. C. *Inorg. Chem.* **1995**, *34*, 4230−4238.
(34) Valencia, L.; Martínez, J.; Macías, A.; Bastida, R.; Carvalho, R. A.; Geraldes, C. F. G. C. *Inorg. Chem.* **2002**, *41*, 5300−5312.

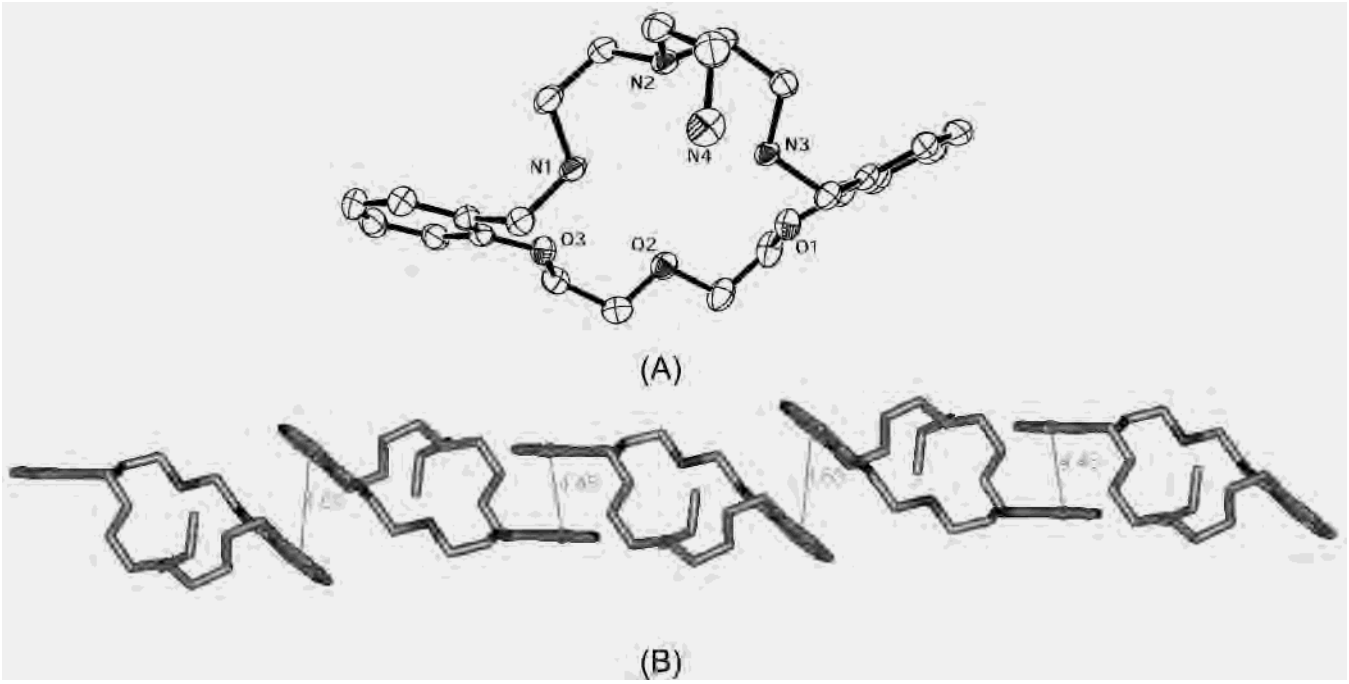

Figure 2. (A) X-ray crystal structure of $[H_2\mathbf{L}](ClO_4)_2 \cdot 3H_2O$ showing 50% probability thermal elipsoids. Hydrogen atoms, solvent molecules, and perchlorate ions have been omitted for simplicity. (B) Perspective view of $[H_2\mathbf{L}](ClO_4)_2 \cdot 3H_2O$ showing a 1D chain. Offset face-to-face $\pi-\pi$ interactions are indicated with a thin line accompanied by the distance centroid···centroid in Å.

slow compared to NMR time scale. Except in the Pb^{2+} titration, the end point is reached at 1:1 (metal:ligand) stoichiometry. The titration with Pb^{2+} shows the presence of two different species depending on whether the metal−ligand stoichiometry is 1:1 or 2:1. ^{1}H NMR spectrum of the first species is exactly the same as the spectrum of synthesized $[Pb\mathbf{L}](ClO_4)_2$ complex. In the course of the experiment part of the $[Pb\mathbf{L}](ClO_4)_2$ complex precipitated as white powder. The ^{1}H NMR spectrum of the second species, which could be formulated as $[Pb_2\mathbf{L}](ClO_4)_4$, was completely assigned using COSY and HMQC spectra (Table S1, Supporting Information). Attempts to isolate $[Pb_2\mathbf{L}](ClO_4)_4$ from solution were unsuccessful; in all cases only a precipitate of $[Pb\mathbf{L}](ClO_4)_2$ could be isolated.

X-ray Structures. The structure of **L** has been determined from a crystal of $[H_2\mathbf{L}](ClO_4)_2 \cdot 3H_2O$. The molecular structure is shown in Figure 2a, and the crystallographic details, with those of the complexes, are summarized in Table 1. The bond lengths and angles in the ligand are normal. The distances N1−C11 = 1.506(5) and N3−C16 = 1.513(5) Å demonstrate that the azometine reduction has taken place. There are many hydrogen bond interactions between the ligand, the three water molecules, and the two perchlorate anions. Each aromatic ring is involved in an offset face-to-face $\pi-\pi$ interaction with rings belonging to neighboring ligands (distance centroid···centroid 4.63 and 4.48 Å, respectively) leading to a supramolecular 1D chain (Figure 2b).[35,36] The interplanar separation and the offset angle between the rings planes are 3.40 Å and 0.0° for the interaction 1 and 3.35 Å and 0.0° for the interaction 2.

Recrystallization of the lead complex from MeCN gave crystals of $[Pb\mathbf{L}](ClO_4)_2$. The molecular structure and selected bond lengths and angles are given in Figure 3A. The structure is formed by coordination of **L** to a single lead ion. The flexibility of the macrocycle allows it to adopt a folded conformation where the Pb ion interacts with all the donor atoms of the ligand. The lead to nitrogen donor atom bond lengths range from 2.487(4) to 2.657(4) Å. The Pb−O distances are longer (similar and of ca. 3 Å; see Figure 3a). These distances are shorter than the Pb−O sum of van der Waals radii (3.8 Å).[37] The coordination number for the Pb atom can be taken as 7 considering the metal−oxygen interactions, and the coordination geometry around lead may be described as holodirected.[38] In the crystalline state, perchlorate anions do not bond the metal (only a weak interaction with one perchlorate can be considered, with a Pb−O1p^i distance of 3.326(6) Å; symmetry operation i transforms as $-x+1, -y, -z$). The distances and angles in the ligand are normal. An aromatic ring experiences an offset face-to-face $\pi-\pi$ interaction with another aromatic ring belonging to a neighboring macrocyclic complex, which leads to a supramolecular dimer (Figure 3B).[35,36] The interplanar separation of the aromatic rings is 3.69 Å (distance centroid···centroid 4.56 Å), and the dihedral angle between the ring planes is 0.0°.

Slow diffusion of a diluted ethanol solution of $Zn(ClO_4)_2 \cdot 6H_2O$ into a $\mathbf{L} \cdot 4HCl$ water solution gave colorless crystals of $[Zn\mathbf{L}Cl](ClO_4).H_2O$. The molecular structure and selected bond lengths and angles are given in Figure 4. The X-ray crystal structure confirms the presence of a mononuclear

(35) Min, K. S.; Suh, M. P. *Eur. J. Inorg. Chem.* **2001**, 449−455.
(36) Jorgensen, W. L.; Severance, D. L. *J. Am. Chem. Soc.* **1990**, *112*, 4768−4774.
(37) Batsanov, S. S. *Russ. J. Inorg. Chem.* **1991**, *36*, 1694−1707.
(38) Shimoni-Livny, L.; Glusker, J. P.; Bock, C. W. *Inorg. Chem.* **1998**, *37*, 1853−1867.

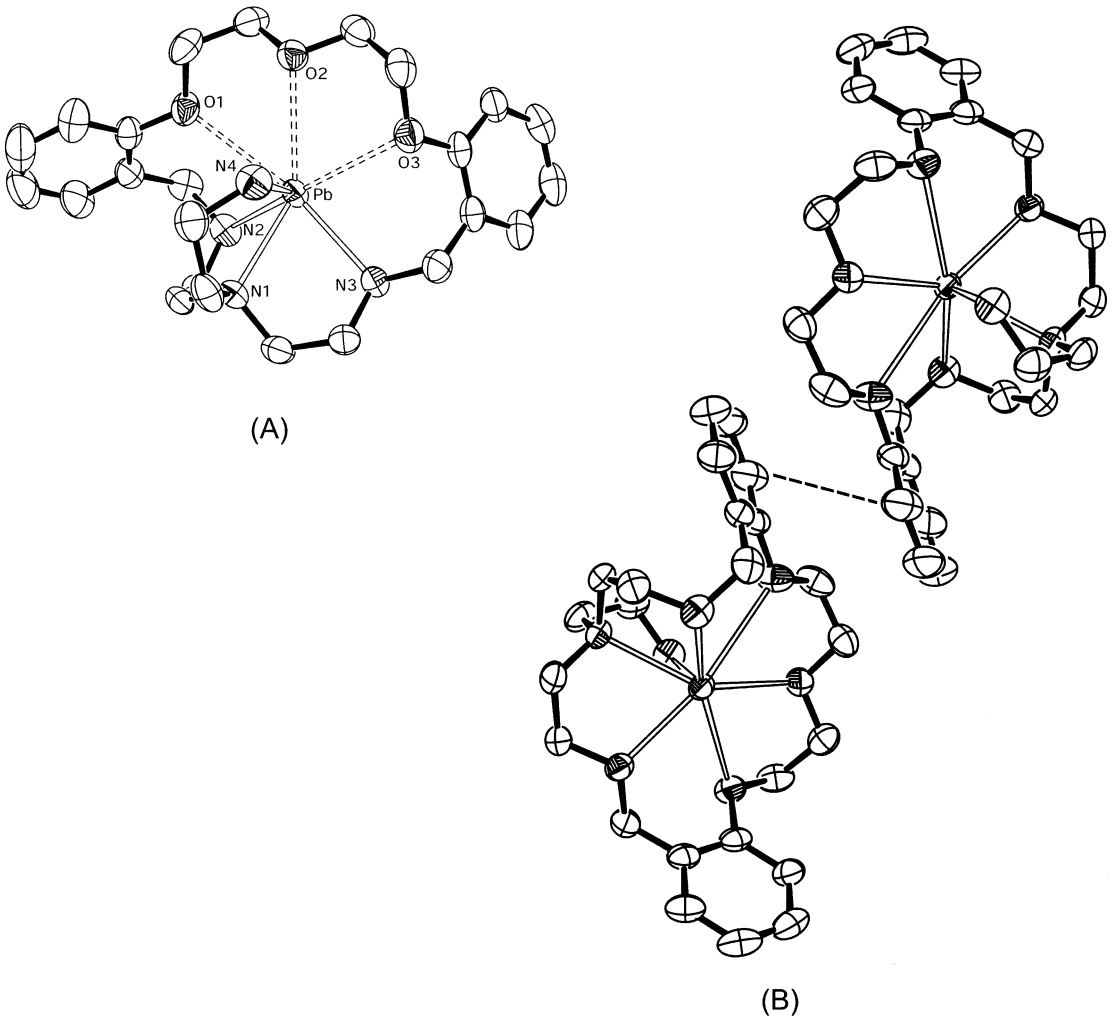

Figure 3. (A) X-ray crystal structure of [Pb**L**]$(ClO_4)_2$ showing 50% probability thermal elipsoids. Hydrogen atoms and perchlorate ions have been omitted for simplicity. Selected bond lengths (Å) and angles (deg) at the metal: Pb−N(4) 2.452(7), Pb−N(3) 2.531(7), Pb−N(1) 2.541(7), Pb−N(2) 2.631(7), Pb−O(1) 2.968(7), Pb−O(2) 3.034(5), Pb−O(3) 2.991(6), N(4)−Pb−N(3) 95.6(2), N(4)−Pb−N(1) 70.15(19), N(3)−Pb−N(1) 71.09(16), N(4)−Pb−N(2) 122.2(2), N(3)−Pb−N(2) 107.54(16), N(1)−Pb−N(2) 68.97(15), C(1)−N(1)−Pb 110.4(3), C(23)−N(1)−Pb 110.3(3), C(22)−N(1)−Pb 108.0(3), C(2)−N(2)−C(3) 115.0(5), C(2)−N(2)−Pb 111.6(3), C(3)−N(2)−Pb 114.6(4), C(21)−N(3)−Pb 111.5(3), C(20)−N(3)−Pb 118.1(4), C(24)−N(4)−Pb 109.5(4). (B) Perspective view of [Pb**L**]$(ClO_4)_2$ showing a dimer. The offset face-to-face $\pi-\pi$ interaction is indicated as a dotted line. Thermal ellipsoids are drawn at the 50% probability level.

complex. The metal atom is pentacoordinated with a distorted trigonal bipyramidal geometry, where the Cl atom of the chloride anion and the tertiary amine nitrogen are the axial atoms. The Zn atom is nearly 0.30 Å below the plane formed by the three equatorial atoms toward the axial Cl atom. The shortest distances are those to the equatorial atoms. The oxygen atoms of the macrocycle do not interact with the metal so that the Zn is very asymmetrically placed in the macrocyclic cavity. Also in the Zn complex, the perchlorate anion does not interact with the metal.

Ligand Protonation. The protonation constants of **L**, reported in Table 2, were determined by potentiometry in 0.15 mol dm^{-3} NaCl, at 298.0 K. Although ligand **L** can bind up to four protons, only three protonation steps could be detected in the pH range used in potentiometric measurements ($2 < pH < 10$). These three protonation constants have rather close values, suggesting that the protons in the species $H_3\mathbf{L}^{3+}$ are far from each other, occupying the primary and the two secondary nitrogens, minimizing in this way the electrostatic repulsion between positive charges. The entrance of a fourth proton to the sterically more protected tertiary nitrogen of the macrocyclic ring, in the middle of three protonated nitrogens, should be difficult due to electrostatic repulsions. And since the protonation of tertiary amines in water is more difficult than secondary and primary amines,[39] the fact that the fourth protonation constant could not be detected in the studied pH range can then be accounted for.

Despite the low value of log K for the last protonation step (log $K < 1.5$), the overall basicity of **L** is somewhat higher ($\Sigma\log K = 27.2$) when compared with *cis*-[18]ane-N_4O_2 ring ($\Sigma\log K = 26.3$).[40] This reflects the presence of the pendant arm that allows the positive charge to spread over a larger volume.

(39) Bencini, A.; Bianchi, A.; Garcia-España, E.; Micheloni, M.; Ramirez, J. A. *Coord. Chem. Rev.* **1999**, *188*, 97−156.
(40) Hancock, R. D.; Bhavan, R.; Wade, P. W.; Boeyens, J. C. A.; Dobson, S. M. *Inorg. Chem.* **1989**, *28*, 187−194.

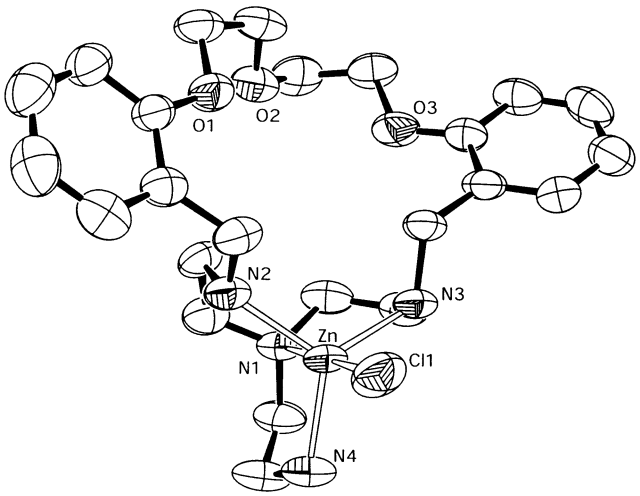

Figure 4. X-ray crystal structure of [Zn**L**Cl](ClO$_4$)·H$_2$O showing 50% probability thermal elipsoids. Hydrogen atoms, solvent molecules, and perchlorate ions have been omitted for simplicity. Selected bond lengths (Å) and angles (deg) at the metal: Zn−N(4) 2.073(5), Zn−N(2) 2.089(5), Zn−N(3) 2.094(5), Zn−N(1) 2.241(5), Zn−Cl(1) 2.371(2), N(4)−Zn−N(2) 117.1(3), N(4)−Zn−N(3) 119.0(3), N(2)−Zn−N(3) 118.0(2), N(4)−Zn−N(1) 81.6(2), N(2)−Zn−N(1) 81.38(19), N(3)−Zn−N(1) 82.4(2), N(4)−Zn−Cl(1) 98.0(2), N(2)−Zn−Cl(1) 98.17(16), N(3)−Zn−Cl(1) 98.47(17), N(1)−Zn−Cl(1) 179.16(14), C(22)−N(1)−Zn 105.4(4), C(23)−N(1)−Zn 105.9(4), C(1)−N(1)−Zn 106.5(3), C(3)−N(2)−Zn 113.4(4), C(2)−N(2)−Zn 110.3(4), C(21)−N(3)−Zn 108.1(4), C(20)−N(3)−Zn 112.2(4), C(24)−N(4)−Zn 110.5(4).

Table 2. Protonation Constants (log K) of Free **L** and Stability Constants with Cu^{2+}, Zn^{2+}, and Cd^{2+} in 0.15 mol dm^{-3} NaCl at 298.0 ± 0.1 K

equilibrium	log K[a]
$\mathbf{L} + H^+ \leftrightarrows H\mathbf{L}^+$	9.735(7)
$H\mathbf{L}^+ + H^+ \leftrightarrows H_2\mathbf{L}^{2+}$	8.76(1)
$H_2\mathbf{L}^+ + H^+ \leftrightarrows H_3\mathbf{L}^{3+}$	7.21(2)
$Cu^{2+} + \mathbf{L} \leftrightarrows Cu\mathbf{L}^{2+}$	17.95(2)
$Cu\mathbf{L}^{2+} + H^+ \leftrightarrows CuH\mathbf{L}^{3+}$	4.12(4)
$Cu\mathbf{L}^{2+} + OH^- \leftrightarrows Cu\mathbf{L}(OH)^+$	9.46(3)
$Zn^{2+} + \mathbf{L} \leftrightarrows Zn\mathbf{L}^{2+}$	12.589(3)
$Zn\mathbf{L}^{2+} + H^+ \leftrightarrows ZnH\mathbf{L}^{3+}$	5.72(1)
$Zn\mathbf{L}^{2+} + OH^- \leftrightarrows Zn\mathbf{L}(OH)^+$	7.833(8)
$Zn\mathbf{L}(OH)^+ + OH^- \leftrightarrows Zn\mathbf{L}(OH)_2$	3.18(1)
$Cd^{2+} + \mathbf{L} \leftrightarrows Cd\mathbf{L}^{2+}$	5.04(2)
$Cd\mathbf{L}^{2+} + H^+ \leftrightarrows CdH\mathbf{L}^{3+}$	9.53(3)
$CdH\mathbf{L}^{3+} + H^+ \leftrightarrows CdH_2\mathbf{L}^{4+}$	8.23(3)
$Cd\mathbf{L}^{2+} + OH^- \leftrightarrows Cd\mathbf{L}(OH)^+$	2.92(3)

[a] Values in parentheses are standard deviations on the last significant figure.

Metal Complex Formation in Aqueous Solutions. The binding properties of **L** toward Cu^{2+}, Zn^{2+}, and Cd^{2+} were studied by potentiometry in 0.15 mol dm^{-3} NaCl, at 298.0 K; the stability constants are presented in Table 2. The complexes that form are characterized by moderate to low solubilities, and in the particular case of Pb^{2+}, no stability data could be obtained by potentiometric methods, since precipitation occurs for pH > 4 ([**L**] = 5.0×10^{-4} mol dm^{-3}, [Pb^{2+}] = 4.0×10^{-4} mol dm^{-3}).

Table 2 also shows that **L** forms only mononuclear complexes with these metal ions and that they are able to protonate and to form hydroxo complexes. The stability constants of the complexes of **L** are low when compared to macrocyclic tetraamine ligands.[41,42] They are close to the constants exhibited by N_4O_2 macrocycles of comparable ring size.[40] For instance, the stability constants of the complexes of Cu^{2+} and Zn^{2+} with [12]ane-N_4 are 23.29[41] and 16.2,[42] respectively, while those with [18]ane-N_4O_2 are 17.85 and 9.52,[40] closer to the log K values of **L** with Cu^{2+} (17.95) and Zn^{2+} (12.589). The N_3O_3 parent macrocycle of **L**, lacking the pendant arm, shows lower stability constants when compared to **L** (log K = 16.5 for Cu^{2+},[43] 9.3 for Zn^{2+},[44] and 8.9 for Cd^{2+};[44] in 0.1 mol dm^{-3} Et_4NClO_4 in 95% MeOH), as would be expected due to the presence of an additional (flexible) nitrogen ligand in **L**. However, the fact that the complexes of **L** form monoprotonated species with relatively high constants may suggest that protonation occurs on a nitrogen atom weakly involved in metal coordination. In the particular case of the complex between **L** and Cd^{2+}, the equilibrium constant for the addition of the first proton (9.53) is only slightly lower than the first protonation constant of free **L** (9.735), indicating that one of the nitrogens is not involved in coordination to the metal center. The detection of a diprotonated complex with a high constant for the entrance of a second proton further suggests that another one of the four nitrogens is only weakly involved in coordination to Cd^{2+}; these observations are in accordance with the low value determined for the stability constant of **L** with Cd^{2+}.

Among macrocycles with pendant arms, the stability constants of **L** with metal ions are close to those reported for a series of [15]ane-N_3O_2 macrocyclic ligands bearing three pendant arms.[45,46] In the particular case of the ligand containing three ethylamino groups as pendant arms, the constants are log K = 17.38, 12.15, and 13.02 (in 0.1 mol dm^{-3} Me_4NCl), respectively, for Cu^{2+}, Zn^{2+}, and Cd^{2+}, which compare well with the values of log K for **L** with Cu^{2+} and Zn^{2+} but not with Cd^{2+}. To account for the higher stability constant with Cd^{2+} relative to Zn^{2+}, the authors suggested[45] an involvement of the oxygens in the coordination of Cd^{2+}. However, that seems not to be the case for the complex of **L** with Cd^{2+}, since the respective stability constant is quite low (log K = 5.04). The crystal structure of the complex of **L** with Pb^{2+} shows that the oxygens are involved in the coordination to this metal ion while the crystal structure with Zn^{2+} shows that this ion is coordinated by the four nitrogens and a chloride ion. Cd^{2+} is larger than Zn^{2+} and smaller than Pb^{2+}; it probably does not fit well into the small cavity made by the four nitrogens, but it is not large enough to be coordinated by the oxygens.

Spectrophotometric and Spectrofluorometric Studies. The absorption and fluorescence emission spectra of compound **L** are reported in Figure 5. Both spectra are similar to those exhibited by the model compound dibenzo-18-

(41) Thöm, V. J.; Hosken, G. D.; Hancock, R. D. *Inorg. Chem.* **1985**, *24*, 3378−381.
(42) Kodama, M.; Kimura, E. *J. Chem. Soc., Dalton Trans.* **1977**, 2269−2276.
(43) Davis, C. A.; Duckworth, P. A.; Leong, A. J.; Lindoy, L. F.; Bashall, A.; McPartlin, M. *Inorg. Chim. Acta* **1998**, *273*, 372−378.
(44) Davis, C. A.; Leong, A. J.; Lindoy, L. F.; Kim, J.; Lee, S.-H. *Aust. J. Chem*. **1998**, *51*, 189−193.
(45) Tei, L.; Blake, A. J.; Bencini, A.; Valtancoli, B.; Wilson, C.; Schröder, M. *J. Chem. Soc., Dalton Trans.* **2000**, 4122−4129.
(46) Tei, L.; Blake, A. J.; Bencini, A.; Valtancoli, B.; Wilson, C.; Schröder, M. *Inorg. Chim. Acta* **2002**, *337*, 59−69.

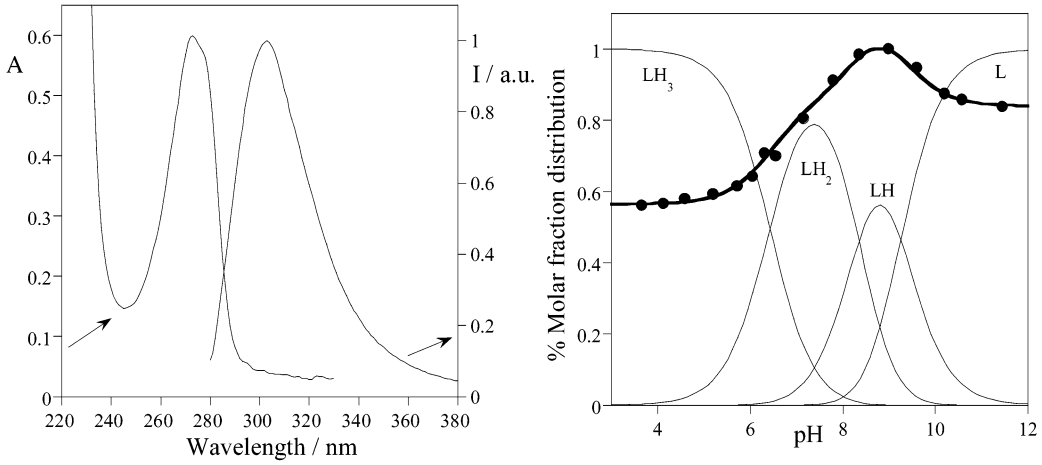

Figure 5. Absorption and emission spectra at the excitation wavelength of 275 nm of **L** (left). Fluorescence emission titration curve of **L** (λ_{exc} = 275 nm, λ_{em} = 303 nm, [**L**] = 4.6 × 10^{-5} M, [NaCl] = 0.15 M), superimposed on the respective mole fraction distribution of the different species present in solution (right).

crown-6, with similar aromatic chromophore units (see Figure S1 in the Supporting Information). The absorption spectrum presents a band at 275 nm which is slightly dependent on the protonation state of the polyamine present on the macrocyclic skeleton (see Figure S2 in the Supporting Information). Protonation of the benzylic amine groups of the macrocycle leads to charge withdrawal from the oxygens due to hydrogen bond formation. As a consequence, a red shift and an increase in the molar absorptivity are observed in the absorption spectra (see Figure S2 in the Supporting Information), in accordance to what is reported to occur in the ^1L_b transition of *p*-cresol.[47]

The emission fluorescence titration (Figure 5) shows a decrease in intensity upon total protonation of the ligand. Since the radiative rate constant, k_f, is expected to be increasing with a decrease in pH (the molar absorptivity coefficient is increasing with a decrease in pH), the results of Figure 5 suggest that the nonradiative rate constant becomes the dominating decay path for the excited state, thus explaining the lower emission intensity at low pH values. At more alkaline pH values, a photoinduced electron transfer from the amine lone pairs to the excited aromatic fluorophore usually takes place in aromatic substituted polyamine receptors.[48] The fluorescence emission titration in Figure 5 results then from a competition between the formation of O···H−N^+ hydrogen bonds at acidic and neutral pH values and photoinduced electron-transfer processes at alkaline pH values.

Metal Complexes. The macrocycle ligand **L** was studied in 0.15 mol dm^{-3} NaCl aqueous solution in the presence of equimolecular amounts of Cu^{2+}, Zn^{2+}, Cd^{2+}, and Pb^{2+}. When the cation employed was Pb^{2+} using nitrate or perchlorate as counterions, a white solid precipitate always formed for pH > 4. This result prevented further studies in solution with this metal by absorption and fluorescence emission.

For the other metal ions, the absorption spectra of the coordination compounds are very similar to that of the free ligand, consisting in a band centered at 275 nm, slightly dependent on pH.

The fluorescence emission titration curves of **L** with Cu^{2+}, Zn^{2+}, and Cd^{2+}, superimposed with the molar fraction distribution curves obtained by potentiometry, are represented in Figure 6.

Concerning the Cu^{2+} complex, a strong CHEQ effect (*chelation enhancement of the quenching*) can be observed. This quenching arises at pH = 4.5 in which the first complex species $[Cu\mathbf{L}H]^{3+}$ is formed. The quenching is totally effective for the $[Cu\mathbf{L}]^{2+}$ and $[Cu\mathbf{L}(OH)]^{+}$ species at neutral and alkaline pH values. This quenching of the fluorescence emission upon Cu^{2+} complexation is commonly observed in polyamine ligands containing aromatic fluorophores and is attributed to an energy transfer quenching of the π^* emissive state though low-lying metal-centered states.[49]

In contrast with Cu^{2+}, the behavior of Zn^{2+} and Cd^{2+} coordinated to polyammonium ligands or in this case to oxoaza macrocyclic ligands is in general as that of emissive species leading to a CHEF effect (*chelation enhancement of the fluorescence emission*).[50,51] This was once more confirmed by the fluorescence emission titration curves reported in Figure 6.

In the case of Zn^{2+}, the CHEF effect is manifested upon pH = 6, where the complex species $[ZnH\mathbf{L}]^{3+}$, $[Zn\mathbf{L}]^{2+}$, and $[Zn(OH)\mathbf{L}]^{+}$ start to be present in solution. The most emissive species are the hydroxo complexes $[Zn(OH)\mathbf{L}]^{+}$ and $[Zn(OH)_2\mathbf{L}]$ that dominate the molar fraction distribution curves for pH > 7. As can be observed in the crystal structure for this metal complex, the Zn^{2+} ion is coordinated by the

(47) Chignell D. A.; Gratzer, W. B. *J. Phys. Chem.* **1968**, *72*, 2934−2941.
(48) Pina, F.; Bernardo, M. A.; García-España, E. *Eur. J. Inorg. Chem.* **2000**, 2143−2157.
(49) Czarnik, A. W. *Fluorescent Chemosensors for Ion and Molecule Recognition*; American Chemical Society: Washington, DC, 1993.
(50) Valeur, B. *Molecular Fluorescence. Principles and Applications*; Wiley-VCH: Weinheim, Germany, 2002.
(51) De Silva, A. P.; Nimal Gunaratne, H. Q.; Gunnlaugsson, T.; Huxley, A. J. M.; McCoy, C. P.; Rademacher, J. T.; Rice, T. E. *Chem. Rev.* **1997**, 1515−1566.

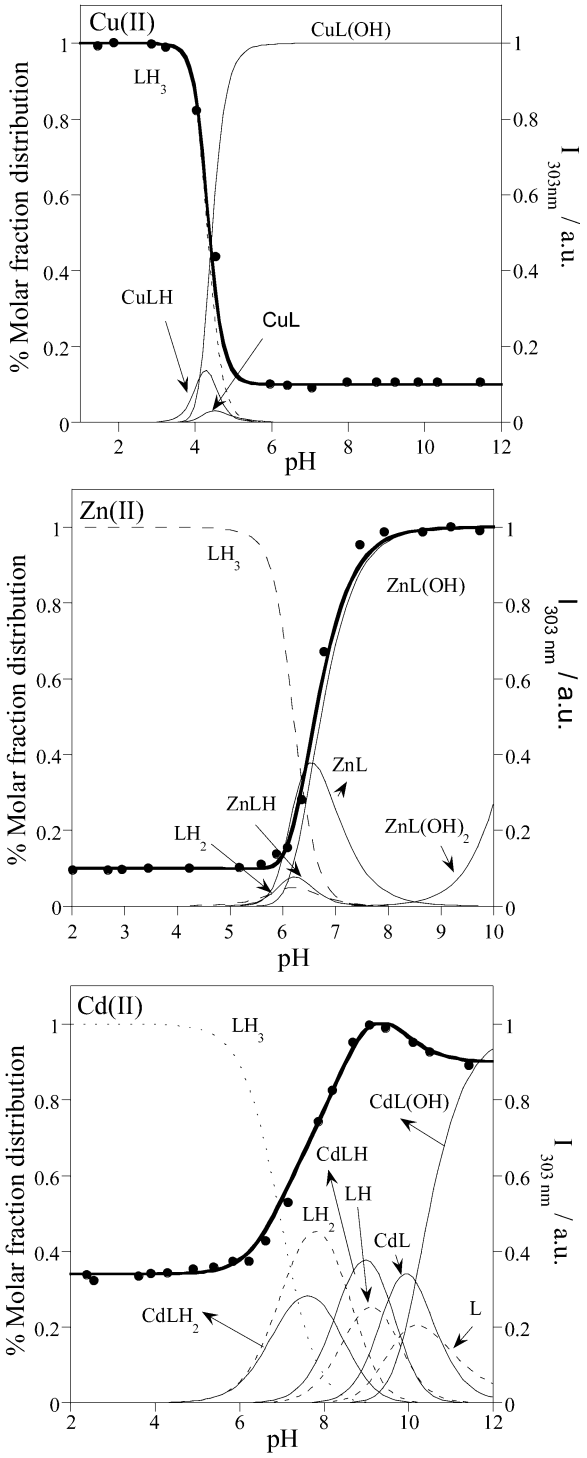

Figure 6. Fluorescence emission titration curves of **L** (λ_{exc} = 275 nm, λ_{em} = 303 nm, [**L**] = 4.95 × 10^{-5} M, [NaCl] = 0.15 M) in the presence of equimolecular amounts of Cu^{2+}, Cd^{2+}, and Zn^{2+} (1:1 molar ratio) as function of pH ([**L**] = [M^{2+}], superimposed on the respective mole fraction distribution of the different species present in solution. Protonated curves are represented as dashed lines, and complexed, as solid lines.

four nitrogens present in the ligand and one chloride anion. After pH = 7, the chloride is probably replaced by a hydroxide anion, precluding any possibility of photoinduced electron transfer. Apparently, the entrance of a second hydroxide anion to form the [$Zn(OH)_2$**L**] species is not

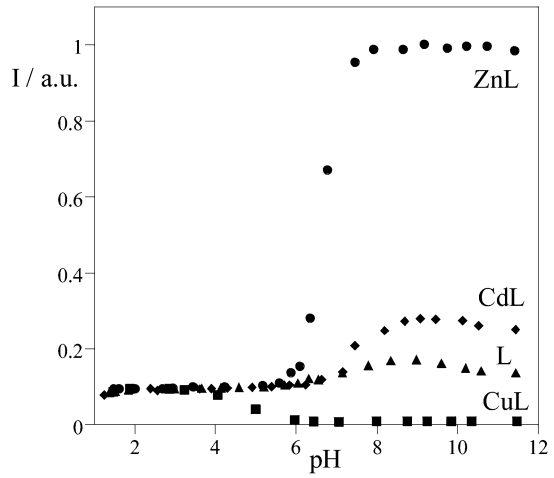

Figure 7. Fluorescence emission titration curves of **L** (▲) in the presence of equimolecular amounts of Cu^{2+} (■), Cd^{2+} (◆), and Zn^{2+} (●) (λ_{exc} = 275 nm, λ_{em} = 303 nm, [**L**] = 4.95 × 10^{-5} M, [NaCl] = 0.15 M).

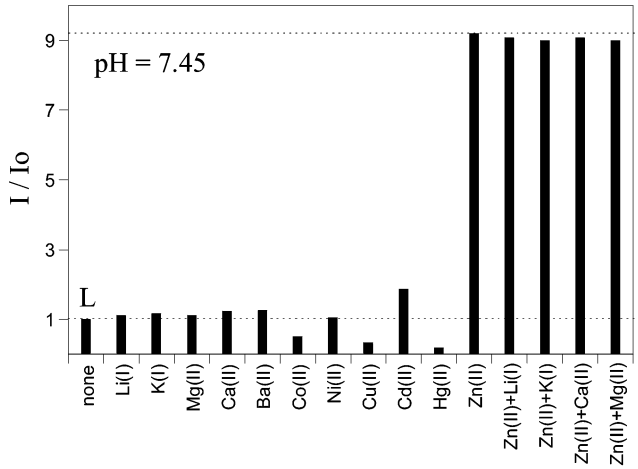

Figure 8. Relative fluorescence intensity at 303 nm of **L** responding to 1 equiv of metal ions at pH 7.45, with I = 0.15 M (NaCl) at 25 °C (excitation at 275 nm). I_o is the emission intensity at 303 nm of **L** (4.70 × 10^{-5} M) in the absence of metal ions at pH 7.45. The presence of an excess amount (up to 1:100) of Li^+, K^+, Ca^{2+}, and Mg^{2+} is represented in the last four columns, respectively.

associated with detachment of any nitrogen since this would in principle lead to a quenching effect that is not observed.

In the presence of Cd^{2+}, the most emissive species are [CdH**L**]$^{3+}$ and [Cd**L**]$^{2+}$, and only a slight quenching is observed for the hydroxo complex [$Cd(OH)$**L**]$^+$. The coordination of Cd^{2+} to **L** is characterized by a low stability constant, and the overall titration curve is very similar to that of free **L**.

Figure 7 compares the titration curves of **L** in the absence and in the presence of three different cations to evaluate the chemosensor ability of the ligand toward Cu^{2+}, Zn^{2+}, and Cd^{2+}. Until pH = 4, only protonated forms of **L** are present in solution and the four titration curves are coincident. After pH = 4, Cu^{2+} can be detected due to the strong CHEQ effect caused by this ion. Between pH = 4 and 6, only Cu^{2+} is detected since the ligand shows a much stronger affinity for this ion relative to the others, as reflected in the stability constants of Table 2. After pH = 6, both Zn^{2+} and Cd^{2+} cause a CHEF effect and can be detected by an increase in

fluorescence emission. But while Cd^{2+} leads to a 1-fold increase in the fluorescence intensity, Zn^{2+} leads to a 10-fold increase.

Selective Metal Signaling of L and Interferences on ZnL Emission. The fluorescence responses of **L** (4.70×10^{-5} M) at pH 7.45 to Zn^{2+}, Cd^{2+}, Cu^{2+}, and other metal ions Li^+, K^+, Mg^{2+}, Ca^{2+}, Ba^{2+}, Co^{2+}, Ni^{2+}, and Hg^{2+} (1 equiv of metal ion, 47 μM) with $I = 0.15$ M (NaCl) at 25 °C (excitation at 275 nm) are summarized in Figure 8. A strong CHEQ effect is observed for Co^{2+}, Cu^{2+}, and Hg^{2+} ions.

The selectivity of **L** toward Zn^{2+} at this pH is very clear. The presence of a huge excess of Li^+, K^+, Mg^{2+}, and Ca^{2+} (up to 1:100) had a negligible effect on the emission of the Zn**L** complex.

Conclusion

We have synthesized a new ligand **L** provided with a flexible amine pendant arm that is an effective complexation agent for several divalent metal ions. Two new crystals structures of [Pb**L**]$(ClO_4)_2$ and [Zn**L**Cl]$(ClO_4)\cdot H_2O$ are also reported, as well as the crystal structure of the $[H_2\mathbf{L}](ClO_4)_2\cdot 3H_2O$. In both complexes, the metal ion is located inside the macrocyclic cavity, having the pendant arm coordinated to the metal center. In the Pb^{2+} complex, the metal is coordinated by all N_4O_3 donor atoms, while, in the [Zn**L**Cl] complex, the metal ion is encapsulated only by the amine atoms present in the ligand. The ligand appears to be very selective for Zn^{2+} at the conditions studied (pH = 7.45, 25 °C, 0.15 M NaCl), in aqueous solution. Two emissive complexes with Zn^{2+} and Cd^{2+} were formed, and the emission remains high at alkaline pH values. The 10-fold increase in fluorescence emission observed in the pH range 7−9 in the presence of Zn^{2+} leads to **L** as a good sensor for this biological metal in water solution.

Acknowledgment. Intensity measurements were performed at Unidade de Raios X, RIAIDT, University of Santiago de Compostela, Santiago de Compostela, Spain, and at the Department of Chemistry, The University of Sheffield, Sheffield, U.K. We are indebted to the European Union Network Contract HPRN-CT-2000-00029 "Molecular Level Devices and Machines", Fundação para a Ciência e Tecnologia POCTI "QUI/32442/99-00" (FEDER), and Xunta de Galicia (PGIDT01PXI20901PR) for financial support.

Supporting Information Available: An X-ray crystallographic file, in CIF format, Table S1, showing ^{1}H and ^{13}C NMR data (500 MHz) in CD_3CN for **L**·MeOH, [Ca**L**]$(ClO_4)_2\cdot 2H_2O$, [Pb**L**]$(ClO_4)_2\cdot$ 0.5EtOH, and $[Pb_2\mathbf{L}](ClO_4)_4$, Figure S1, showing absorption and emission spectra at the excitation wavelength of 275 nm of the parent compound dibenzo-18-crown-6, and Figure S2, showing the absorption spectra of **L** as function of pH and absorption at 275 nm and emission at 303 nm ($\lambda_{exc} = 275$ nm) of the ligand **L**. This material is available free of charge via the Internet at http://pubs.acs.org.

IC034245Z